Infrared Light-Active Shape Memory Polymer Filled with Nanocarbon Particles

Jinsong Leng,[1] Xuelian Wu,[1] Yanju Liu[2]

[1]*Center for Composite Materials and Structures, Science Park of Harbin Institute of Technology (HIT), Harbin, People's Republic of China*
[2]*Department of Aerospace Science and Mechanics, Harbin Institute of Technology (HIT), Harbin, People's Republic of China*

Received 19 November 2008; accepted 7 May 2009
DOI 10.1002/app.30724
Published online 7 July 2009 in Wiley InterScience (www.interscience.wiley.com).

ABSTRACT: In addition to the fabrication of thermoset styrene-based shape memory polymer (SMP) and its nanocomposite filled with nanocarbon particles, this study presents the effect of nanocarbon particles on infrared light-active shape recovery behaviors of this type of SMP material. The experimental results reveal that both pure SMP and SMP filled with nanocarbon particles can be actuated by infrared light in vacuum, while shape memory effect shown by the composite is stronger than that of in pure SMP. Shape memory effect is evaluated by shape recovery ability and shape recovery speed in detail. Moreover, factors which would influence the infrared light-active shape memory effect in SMP with/without nanocarbon particles are explored by scanning electron microscopy (SEM), differential scanning calorimetry (DSC), dynamic mechanical analysis (DMA), and infrared absorption characteristic tests. The better shape memory effect of the nanocomposite attributes to its higher storage modulus and higher infrared absorption capability. © 2009 Wiley Periodicals, Inc. J Appl Polym Sci 114: 2455–2460, 2009

Key words: shape memory polymer; nanocomposite; actuation; infrared light

INTRODUCTION

Shape memory polymer (SMP) is a kind of novel smart material for its outstanding ability to be actuated from a temporary shape into original shape, i.e. shape memory effect, while being heated to a certain temperature. Compared to shape memory alloy, SMP has advantages of large recoverable strain (over 400%), excellent structural versatility, low manufacturing cost, low weight, and ease manufacturing.[1–3] Moreover, composites of SMP reinforced by different fillers have been developed to improve the mechanical, electrical, and magnetic property of SMP. Carbon particles, carbon fibers, carbon nanotube, and magnetic particles, etc. have been used as fillers by many researchers.[4–8] As SMP materials can change their shape and stiffness according to external stimulus, they can be used in many potential smart material applications, such as biomedical devices[9,10] and spatial deployment structure.[11] However, SMP materials have not fully exerted their technological potential applications largely because of the limited actuation methods. Huang et al.[12–14] demonstrated polyurethane SMP could be triggered with water by immersion of the SMP in water. Mohr et al.[8,15] introduced the magnetically induced shape-memory effect of composites from magnetic nanoparticles and thermoplastic SMP. Leng et al.[16–18] demonstrated that the electrical conductivity of the SMP composite can be improved significantly, which makes it more suitable for joule heat induced shape recovery. In these research mentioned earlier, SMP materials were immersed in water or induced by magnetic field or current flow to exhibit shape memory effect, however, some SMP structural components[11] cannot work after immersing in water or interfered by intense magnetic field or current flow. Therefore, it is significant to exploit new actuation method for SMP materials to expand their applications. The infrared light possesses wide emission spectra and unique heating effect in a noncontact manner, therefore actuating SMP materials with infrared light may realize the applications of SMP practically and dramatically.

In this article, in addition to the fabrication of one-way styrene-based SMP and its composite containing 10 wt % carbon nano-particles, infrared light-active shape memory effect of these materials are investigated, and factors which would influence infrared light-active shape memory effect are also explored by infrared absorption characteristic tests, scanning electron microscopy (SEM), differential

Correspondence to: J. S. Leng (Lengjs@hit.edu.cn).

scanning calorimetry (DSC), and dynamic mechanical analysis (DMA).

EXPERIMENTAL PART

The polymer used in this study was a thermoset styrene-based SMP with a density of 0.90 g/cm^3, which was bought from Cornerstone Research Group (CRG). The styrene-based SMP consists of two parts: styrene-based resin and hardener, and the weight ratio of resin and hardener is 28 : 1. The main components of the resin are styrene monomer and styrene block copolymer, and that of the hardener are dibenzoyl peroxide and tricresyl phosphate. The uncrosslinked styrene-based resin was reacted with the hardener which serves as crosslinker during curing process, thereby, the styrene-based shape memory network was formed by the crosslinking polymerization of the resin and the hardener. Carbon nanoparticle (carbon black, CB) with an average particle size of 40 nm and density of 1.81 g/cm^3 was used to prepare SMP/CB composite.

To fabricate styrene-based SMP, after mixing styrene-based resin and hardener, degassing was carried out in a vacuum furnace, and then the liquid was cast into a plate mold for curing in an oven at 75°C for 36 h. Styrene-based SMP nanocomposite filled with 10 wt % of CB was prepared in the following steps. First, CB was added into the resin, which is less viscous than the hardener at room temperature. After that, both mechanical blending and ultrasonic mixing were used to mix the filler and the resin. Subsequently, the hardener was added into the mixture and stirred well. Then, the composite precursor was degassed, cast, and cured using the same process as the SMP resin. After curing, SMP and SMP/CB nanocomposite plates were released from the molds and machined to a bar shape with dimension of approximately 8 × 1 × 0.4 cm^3.

Shape memory cycle includes two steps: predeformation and recovery. A specimen was heated to 90°C which is about T_g + 30°C, and bending was accomplished. After cooling, the bent sample was triggered subsequently for shape recovery. In this article, a new actuation method of infrared light in vacuum was proposed, and a special setup was designed to supply infrared light radiation in vacuum shown in Figure 1. A quartz glass bottle sealed with a rubber stopper was used to supply the vacuum environment. Vacuum pipe and thermocouple sensor were plugged into the glass bottle through holes in the rubber stopper. Infrared light radiator is made up of quartz infrared strip lamp and has a total power-handling capability of 2400 W. Temperature can be adjusted by a power-controller in the infrared actuation setup. The infrared light radiator emits over a broad band of the spectrum from

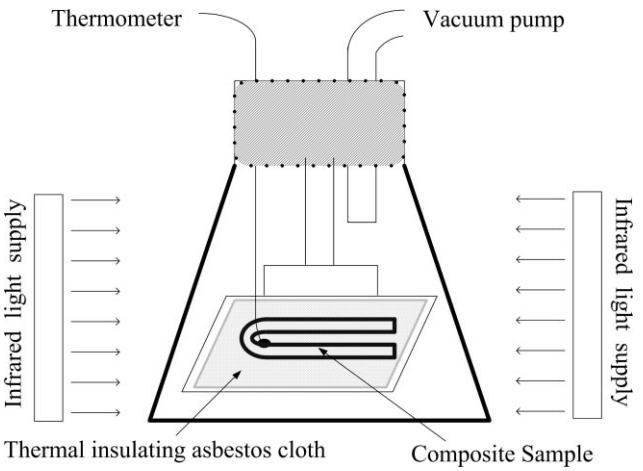

Figure 1 Illustration of actuation setup with infrared light in vacuum.

2.5 μm to 8 μm and the vacuum pressure is −101.325 KPa. In testing, a bent sample fixed in an adiabatic clamp (with thermal insulating asbestos cloth) was placed in the quartz bottle. During the recovery process, digital camera was used to record time against recovery angles.

Absorption capability of SMP and SMP/CB nanocomposite for infrared light were investigated with nicolet 8700 in wave number ranges of 400–4000 (cm^{-1}), and the dimension of sample is 2 × 2 × 0.4 cm^3. Scanning electron microscopy (SEM) (JEOL, JSM-5600LV) was carried out to investigate the distribution of CB in SMP/CB nanocomposite. Glass transition temperature (T_g) of styrene-based SMP and SMP/CB nanocomposite were investigated to set actuation temperature by using differential scanning calorimetry (DSC) (NETZSCH DSC 204F1). Dynamic Mechanical Analysis (DMA) was used to determine the thermomechanical properties of SMP and SMP/CB nanocomposite.

RESULTS AND DISCUSSIONS

Infrared absorption characteristic

The capability to absorb infrared light is determined by molecular (or atom) constitution of materials, because infrared light was absorbed in the form of molecule (or atom) resonance vibration. Absorption spectrum therefore reflects the resonance behavior of molecular (or atom) groups.[19] Figure 2 shows the difference of infrared absorbing efficiency between SMP and SMP/CB composite from 500 to 4000 cm^{-1} in wavenumber. As is shown in the figure, SMP shows obvious absorption (above 3%) in wave number ranges of 450–1960 cm^{-1} and 2760–3130 cm^{-1} with three sharp peaks at 1060, 1830, and 2856 cm^{-1}, and at two of which infrared-absorption strength of SMP is above 5%. While SMP/CB nanocomposite

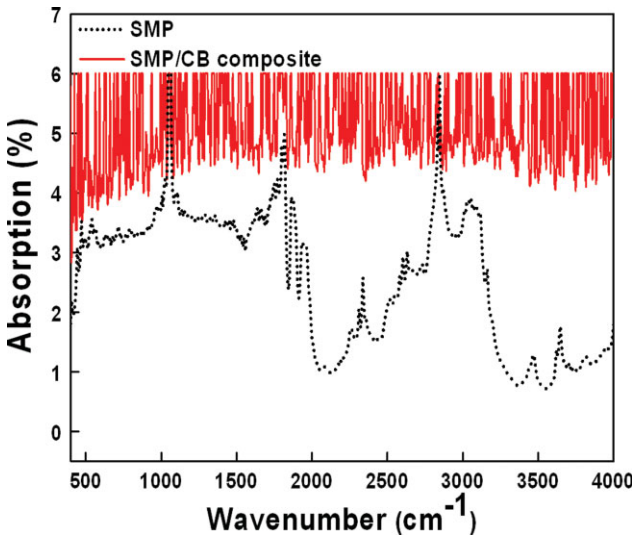

Figure 2 Spectra of infrared-absorption of SMP and SMP/CB composite in range of 400–4000 (cm^{-1}). [Color figure can be viewed in the online issue, which is available at www.interscience.wiley.com.]

shows continuum strong (above 5%) absorption in the whole test wavenumber range. It is apparent that not only the absorption spectrum of the nanocomposite is more wide-range but also the absorption of the nanocomposite is higher than that of the pure SMP. It can be concluded that the existence of CB particles increases the capability to absorb infrared light energy for the composite remarkably.

The absorption for infrared light was determined by the structure of materials. The absorption for infrared light of the pure SMP is determined by the character groups of the polymer, which shows obvious absorption in certain wave number ranges during 500–4000 wavenumbers (cm^{-1}). While, the SMP/CB nanocomposite are composed of two components—the polymer and CB. CB can absorb infrared radiation mostly and remarkably during 500–3000 wavenumbers (cm^{-1}),[20] which increases the absorption for infrared light of the composite remarkably in the whole testing wavenumber range. In cotrast, when SMP and SMP/CB nanocomposite are exposed to infrared light, most of the emitted energy[21,22] is transmitted by SMP which is transparent, while most of the emitted infrared light is absorbed by the nanocomposite since it is black and opaque. In addition, SMP and the nanocomposite have equal reflection approximately beacause their surfaces are similarly smoothness. So, the black CB absorbs infrared radiation much notably than that of pure SMP. Infrared light is unique in that it exhibits heating effect. Previous study has proved that CB can absorb infrared radiation remarkably and produce notable heating effect during 500–4000 wavenumbers (cm^{-1}).[20] In SMP/CB nanocomposite, as light is absorbed, heat is generated by the CB to be released into the matrix (polymer) efficiently. Then, the high capability to absorb infrared light in the nanocomposite will result in the more heat generated.

In this study, based on infrared absorption characteristic of SMP materials, a setup is designed to accomplish the thermo-actuation method of infrared light in vacuum. The infrared actuation is implemented in vacuum condition which can decrease the thermal inertia. Infrared radiation ranged from 2.5 μm to 8 μm is adopted, which is the strongly absorbing region for most of polymers. Besides, infrared heating is realized in the form of electromagnetic radiation, then, the actuation method is noncontact. Therefore, infrared light-actuation method for SMP materials is applicable for almost polymeric materials, making it possible to widen the application of SMP material in the future.

SEM observation

In this study, CB with a content of 10 wt % was chosen to support a homogeneous distribution within the polymer matrix, and SEM was used to observe the dispersion of CB within SMP/CB nanocomposite. As shown in Figure 3, a homogeneous distribution of CB within the composite is achieved with particles embedded in the matrix. As shown in the image, the dark phase corresponds to CB and the light one to styrene-based SMP matrix. As a result, the infrared light could be absorbed uniformly by the nanocomposite in view of the strong capability to absorb infrared light of CB.

Glass transition temperature

T_g is one of the major characteristics of SMP and its composite. Traditionally, T_g can be defined in various ways. Here, Differential scanning calorimetry

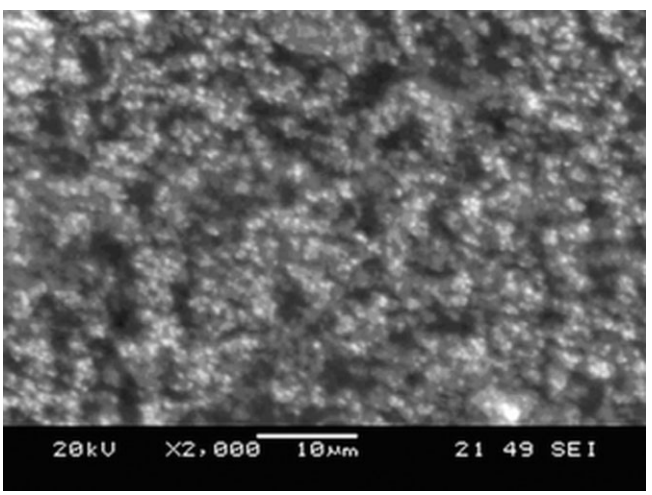

Figure 3 SEM image of SMP/CB composite with the filler content of 10 wt %.

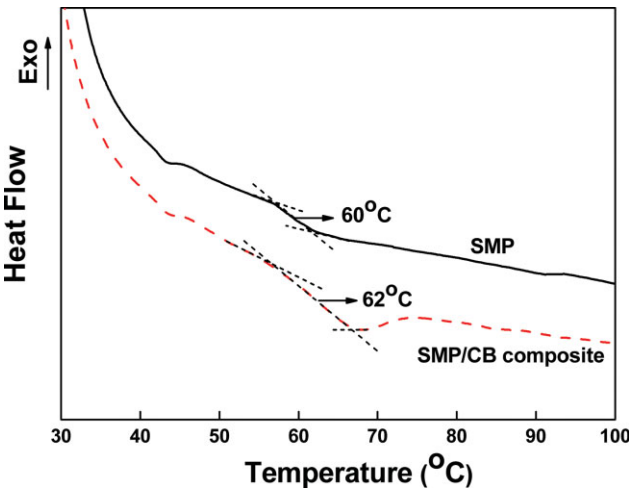

Figure 4 DSC curves of SMP and SMP/CB composite. [Color figure can be viewed in the online issue, which is available at www.interscience.wiley.com.]

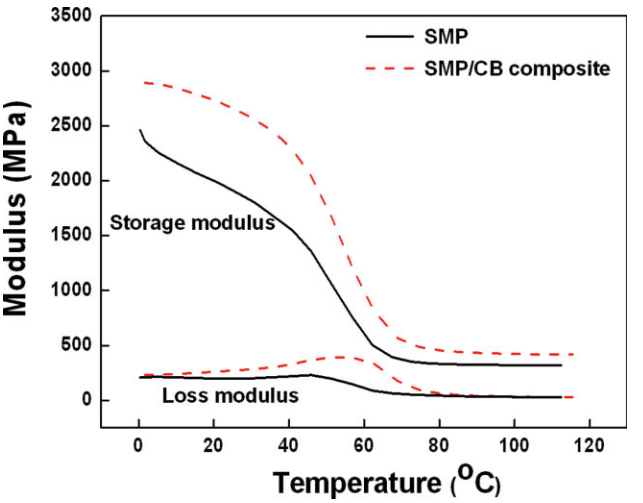

Figure 5 DMA results of SMP and SMP/CB composite. [Color figure can be viewed in the online issue, which is available at www.interscience.wiley.com.]

(DSC) tests were performed on samples to define its T_g using NETZSCH from 20 to 100°C at a constant heating rate of 10°C/min. The full DSC term curves are plotted in Figure 4, in which T_g is determined as 60°C for SMP, 62°C for SMP/CB nanocomposite. According to the DSC results, the T_g increases slightly with the existence of 10 wt % CB. A similar phenomenon has been reported in other polymer composites filled with nano-particles e.g. Ref. 5. A possible explanation is that the possible chemical changes in the polymer near the polymer/particle interface can influence the T_g of the nanocomposites.[5]

Dynamic mechanical analysis (DMA)

The thermomechanical properties of SMP and SMP nanocomposite were investigated by DMA test. The relationship between the dynamic stress and the corresponding strain provides the complex modulus with a real part E_r (storage modulus) and imaginary part E_i (loss modulus). DMA tests were carried out in the three-point bending mode at a heating rate of 10.0 K/min from 0 to 120°C with a frequency of 1 Hz. The storage modulus and loss modulus are recorded against the temperature as shown in Figure 5. At room temperature of 25°C, the storage modulus is 1.9 GPa for SMP and is 2.5 GPa for the nanocomposite. The storage modulus of SMP and the nanocomposite decrease sharply in the temperature range from 40 to 60°C. Storage modulus for the SMP nanocomposite is higher than that of the pure SMP resin within the whole testing temperature range. Because the storage modulus reveals the stiffness of material, it can be obtained that the stiffness of SMP/CB nanocomposite is higher than that of the pure SMP. The increase in stiffness is due to the higher elastic modulus of the CB reinforcement compared to that of the SMP matrix.

In addition, the peak of loss modulus versus temperature curve can be used to define T_g in DMA test, and T_g is found to be 51°C for SMP and 58°C for the nanocomposite from Figure 5. T_g of SMP nanocomposite determined by loss modulus is higher than that of pure SMP, which is consistent with the result from DSC.

Shape memory effect

In this study, shape memory effect is evaluated by shape recovery ability and shape recovery speed. Shape recovery refers to the heated recovery and shape recovery angle is the instantaneous "angle" in recovery which is determined by measuring the angle between the straight ends of the bent specimen as shown in Figure 6. Where, r denotes the radius of mandrel, t represents the thickness of SMPC specimen, R is shape recovery ratio, θ is shape recovery

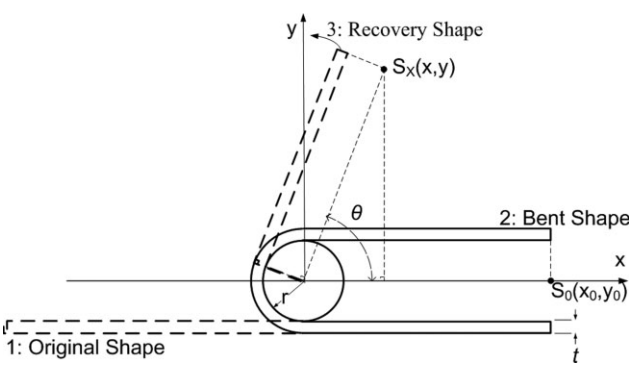

Figure 6 Schematic illustration of shape recovery performances test.

Figure 7 Illustration of shape recovery process in SMP and SMP/CB composite.

angle and it is determined by the selected point S_x (x, y):

$$\theta = \mathrm{ArcCot}\left(\frac{x}{y}\right) \qquad 0^\circ \le \theta \le 180^\circ \tag{1}$$

$$R = \frac{\theta}{180^\circ} 100\% \tag{2}$$

θ and R are obtained through eqs. (1) and (2). In the following tests, the radius r of mandrel and thickness t of SMPC specimen are 3 mm and 4 mm, respectively. Figure 7 is an illustration of recovery process of 100% in shape recovery ratio for the styrene-based SMP and its nanocomposite containing 10 wt % CB used in the study.

The heating temperature range for shape memory effect was set from 50 to 120°C, which is from T_g– 10°C to T_g + 60°C for SMP and the nanocomposite approximately. Figure 8 plots shape recovery ratio versus temperature relations of SMP and SMP/CB nanocomposite. It can be seen that shape recovery ratio is 100% for SMP when temperature is greater than or equals to 80°C which is about 20°C above its T_g (60°C). The full recovery is observed for nanocomposite at/above 70°C, which is about 8°C above its T_g (62°C). The lowest heating temperature corresponding to full recovery for the nanocomposite is lower than that of SMP. In addition, when temperature is below 70°C, both SMP and the nanocomposite cannot recover entirely and shape recovery ratio of the nanocomposite is obviously higher than that of pure SMP. It can be concluded from the above results that the nanocomposite is not only heated easily but also has better shape recovery ability than that of SMP with infrared light-based heating.

Shape recovery speed is an important characteristic for the application of SMP materials. Figure 9 shows the curves of shape recovery angle against time for SMP and SMP/CB nanocomposite at 90°C. Shape memory cycle of each material was repeated five times to investigate the repeatability of shape memory speed. Repeatability test for shape recovery speed is necessary to insure stability of shape recovery effect for SMP materials, because macromolecular material is liable to fatigue in using. As shown in Figure 9, the five parallel test curves corresponding to SMP are uniform regularity, in which the maximum error is 10 seconds; while curves corresponding to the nanocomposite have similar distribution but coincide less compared that of SMP, in which the maximum error is 15 s. The information above shows repeatability of shape recovery speed for SMP and the nanocomposite are similarly good under the actuation of infrared light in vacuum. The good repeatability of shape recovery speed in the nanocomposite attributes to homogeneous dispersion of CB, which has been demonstrated by SEM.

As can be seen from Figure 9, shape recovery speed of the nanocomposite is quicker than that of SMP not only in the whole recovery but also in the recovery

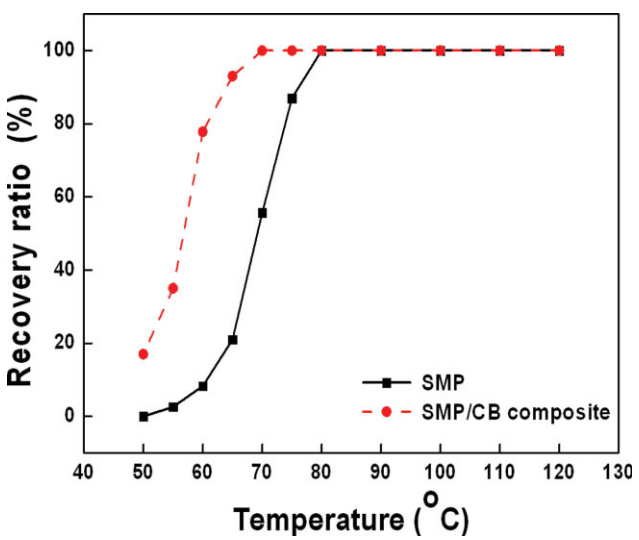

Figure 8 Shape recovery ratio vs temperature relationship of SMP and SMP/CB composite. [Color figure can be viewed in the online issue, which is available at www.interscience.wiley.com.]

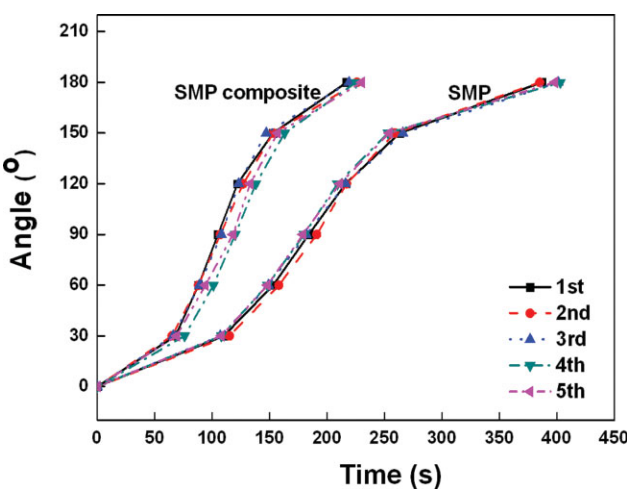

Figure 9 Recovery angle vs time relationship of SMP and SMP/CB composite. [Color figure can be viewed in the online issue, which is available at www.interscience.wiley.com.]

from 30° to 150°. In addition, a close look at Figure 9 shows that changing regularity of shape recovery speed for SMP and the nanocomposite is similar as the following: recovery angle increases almost linearly with time in recovery process from 30° to 150°, but the increasing is slackened as draw near to the angle of 180° from 150°, which is similar to the angle range from 0° to 30°. In brief, it is apparent that shape recovery speed in angle range from 30° to 150° is approximate and quicker than that in the angle ranges from 0°to 30°and from 150° to 180°for each material.

There is a network structure formed by macromolecular chains in thermoset SMP, and the relative motion of macromolecule segment is the primary mechanism of shape memory effect in SMP. In the present styrene-based SMP, the macromolecule segments entangle together randomly before deformation, which is higher in entropy. After predeformation (heating, bending and cooling), the entangled molecule chain of SMP is in an orderly arrangement, which is a metastable structure with low entropy. The strain energy is stored by the constraining effect of the SMP matrix, which is frozen in the bend shape by the transitory molecular interactions. Upon subsequent heating, the stored internal energy was released in the form of recovery force and low entropy state drive individual chains toward their initial state, facilitating shape memory. As shown by the result of DMA, the stiffness of SMP/CB nanocomposite is higher than that of the pure SMP, and the increased stiffness in SMP nanocomposites is critical for the enhanced recoverable stress levels during shape recovery deployment.[23] Therefore, the higher shape recovery force ensures SMP/CB nanocomposite has better shape recovery ratio and can recover its initial shape more easily compared with that of SMP at the same temperature, since the difference of T_g between SMP and the nanocomposite is slight. On the other hand, as shown in the infrared absorption characteristic test, the nanocomposite has a higher capability to absorb infrared radiation compared that of SMP, which is beneficial to improve shape memory effect in the nanocomposite too. Taking into account these factors, the additive of CB not only increase the recovery force but also enhance the capability to absorb infrared light for SMP/CB nanocomposite. Therefore shape recovery ability is better and shape recovery speed is much quicker in the nanocomposite than that in pure SMP.

CONCLUSIONS

Infrared light actuation (in vacuum) method for SMP materials may have a variety of applications in the future, owing to its notable thermal effect. In contrast to what was reported in literatures,[8,15–17] from this study, it is found that not only the nanocomposite but also pure SMP can be actuated by infrared light (in vacuum) in a noncontact manner. Furthermore, the effect of Carbon nano-particle (carbon black, CB) on infrared light-active shape memory effect was investigated by comparing shape memory effect in SMP with/without CB. Shape memory effect is quantified by shape recovery ability and shape recovery speed. The results show that shape memory effect in SMP/CB nanocomposite is better than that of pure SMP, which can be explained by the aforementioned experimental results. In infrared absorption characteristic test, SMP/CB nanocomposite has much stronger absorption compared that of pure SMP for infrared light of 400–4000 wavenumbers (cm^{-1}). In DMA test, CB increases the modulus of the nanocomposite, which may enhance recoverable stress levels during recovery. These factors enhance shape memory effect of the nanocomposite. This approach, i.e., to actuate styrene-based SMP and its nanocomposite containing CB by infrared light in vacuum, is easy for implementation, and it should be applicable to other types of SMP and their composite containing various fillers.

References

1. Behl, M.; Lendlein, A. Mater Today 2007, 10, 20.
2. Andreas, L.; Steffen, K. Angew Chem Int Ed 2002, 41, 2034.
3. Huang, W. M.; Lee, C. W.; Teo, H. P. J Intell Mater Syst Struct 2006, 17, 753.
4. Leng, J. S.; Lv, H. B.; Liu, Y. J.; Du, S. Y. J Appl Phys 2008, 104, 104917.
5. Liu, Y. P.; Gall, K.; Dunn, M. L.; Mccluskey, P. Mech Mater 2004, 36, 929.
6. Beloshenko, V. A.; Varyukhin, V. N.; Voznyak., Y. V. Compos A 2004, 65.
7. Cho, J. W.; Kim, J. W.; Jung, Y. C.; Goo, N. S. Macromol Rapid Commun 2005, 26, 412416.
8. Mohr, R.; Kratz, K.; Weigel, T.; Lucka-Gabor, M.; Moneke, M.; Lendlein, A. Proc Natl Acad Sci USA 2006, 103, 3540.
9. Karp, J. M.; Langer, R. Curr Opin Chem Biol 2007, 18, 454.
10. Lendlein, A.; Langer, R. Science 2002, 296, 1673.
11. Gall, K.; Mikulas, M.; Munshi, N. A.; Beavers, F.; Tupper, M. J Intell Mater Syst Struct 2000, 11, 877.
12. Huang, W. M.; Yang, B. Appl Phys Lett 2005, 86, 114105-1-3.
13. Yang, B.; Huang, W. M. Smart Mater Struct 2004, 13, 191.
14. Leng, J. S.; Lv, H. B.; Liu, Y. J.; Du, S. Y. Appl Phys Lett 2005, 86, 114105-1-2.
15. Buckley, P. R.; Mckinley, G. H.; Wilson, T. S. IEEE Trans Biomed Eng 2006, 53, 2075.
16. Leng, J. S.; Lan, X.; Huang, W. M. Appl Phys Lett 2008, 92, 014104-1-3.
17. Leng, J. S.; Lv, H. B.; Liu, Y. J.; Du, S. Y. Appl Phys Lett 2007, 91, 144105-1-3.
18. Leng, J. S.; Huang, W. M.; Lan, X.; Liu, Y. J.; Liu, N.; Phee, S. Y.; Du, S. Y. Appl Phys Lett 2008, 92, 204101-1-3.
19. Bednarczyk, H.; Buhler, J. Opt Lasers Eng 1995, 22, 271.
20. Fu, F. F.; Watanabec, K.; Shinohara, N.; Xu, X. Q.; Xu, L. J.; Akagi, T. Sci Total Environ 2008, 393, 273.
21. Tjahjono, I. K.; Bayazitoglu, Y. Int J Heat Mass Transfer 2008, 51, 1505.
22. Ryer, A. Light Measurement Handbook; International Light Inc: Newburyport, 1998.
23. Gall, K.; Dunn, M. L.; Liu, Y. P. Appl Phys Lett 2004, 85, 290.